Journal of Hazardous Materials 497 (2025) 139583

Contents lists available at ScienceDirect

Journal of Hazardous Materials

journal homepage: www.elsevier.com/locate/jhazmat

Asbestos identification in bulk samples using FTIR and multivariate data analysis

Salman Alquwayi [a,b], Cody Wolfe [a], Sena Yang [a], Bryan Bandli [c], Steven E. Mischler [a], Taekhee Lee [a,*]

[a] Health Hazards Prevention Branch, Pittsburgh Mining Research Division, National Institute for Occupational Safety and Health, Centers for Disease Control and Prevention, Pittsburgh, PA 15236, USA
[b] University of Pittsburgh, School of Public Health, Department of Environmental and Occupational Health, Pittsburgh, PA 15261, USA
[c] RJ Lee Group, Inc., Monroeville, PA 15146, USA

HIGHLIGHTS

- A laboratory procedure for asbestos identification in asbestos containing materials (ACMs) was developed using FTIR and Partial Least Squares-Discriminant Analysis (PLS-DA).
- The prediction of the PLS-DA model was evaluated using laboratory-generated asbestos-containing samples and suspected ACMs.
- Predicted asbestos type(s) from the PLS-DA model was compared to the results of standard polarized light microscope analysis

GRAPHICAL ABSTRACT

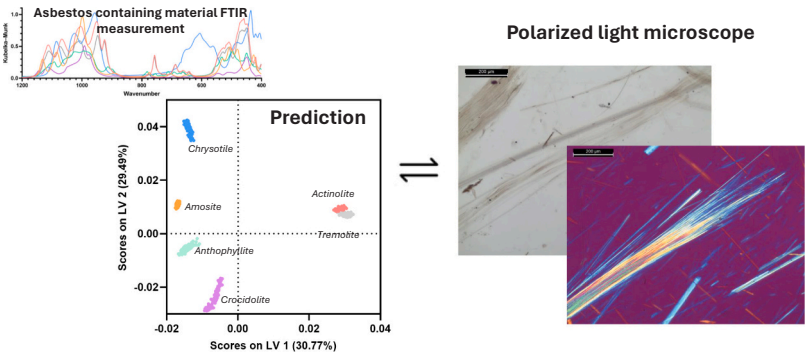

ARTICLE INFO

Keywords:
Bulk asbestos sample analysis
Asbestos containing material
FTIR
Partial least squares-discriminant analysis

ABSTRACT

This study aimed to investigate a laboratory procedure for identifying asbestos in asbestos-containing materials (ACMs) using Fourier Transform Infrared (FTIR) spectroscopy combined with Partial Least Squares-Discriminant Analysis (PLS-DA). A PLS-DA model was trained with the six regulated asbestos reference materials using FTIR with the diffuse reflectance infrared Fourier transform (DRIFT) technique to identify asbestos type(s) in unknown samples. The prediction of the PLS-DA model was evaluated using laboratory-generated asbestos-containing samples and suspected ACMs collected from the remediation and building management industries. Predicted asbestos type(s) from the PLS-DA model in the suspected ACMs were compared to the results of standard polarized light microscope (PLM) analysis. The PLS-DA model predicted 100 % correct classification in laboratory-generated single asbestos-containing samples (n = 30) and 80 % correct classification in mixed-asbestos samples (n = 45). The model predicted 96 % (24/25) correct classification in chrysotile containing bulk samples with extra sample treatment steps (ashing and acid washing). The PLS-DA model prediction with the samples containing multiple asbestos types was less accurate and will require further optimization through

* Correspondence to: Health Hazards Prevention Branch, Pittsburgh Mining Research Division, National Institute for Occupational Safety and Health, 626 Cochrans Mill Road, Pittsburgh, PA 15236, USA.
E-mail address: fwc8@cdc.gov (T. Lee).

https://doi.org/10.1016/j.jhazmat.2025.139583
Received 29 May 2025; Received in revised form 29 July 2025; Accepted 15 August 2025
Available online 16 August 2025
0304-3894/Published by Elsevier B.V.

expanded datasets and model refinement. The proposed method is cost-effective, rapid, and may reduce reliance on the analyst's experience by directly measuring the distinctive chemical properties of the asbestos.

1. Introduction

On March 18, 2024, the United States Environmental Protection Agency (EPA) announced a rule to ban ongoing uses of chrysotile asbestos, motivated in part by the estimated 40,000 asbestos-related deaths occurring annually in the U.S. alone [1]. This regulatory action highlights the continuing need for accurate identification methods for asbestos in materials. Additionally, over 125 million workers worldwide are exposed to asbestos in their workplaces [2], and 232,000 deaths each year are estimated [3]. The adverse health effect due to asbestos exposure has a significant impact on public health systems [4–8] and is considered to be the "largest single cause of occupational cancer" in the US [9]. Asbestos has been used in many applications or types of products for industrial and commercial use. The applications in which asbestos has been used in cement, plastics, resins, roofing, thermal and electrical insulation, cement pipe and sheets, flooring, gaskets, friction materials, coating and compounds, textiles, paper, mastics, thread, fiber jointing, and millboard [10]. Given the substantial health impact and widespread use of asbestos-containing materials (ACMs), the development of improved analytical methods for asbestos fibers and other elongate mineral particles (EMPs) is recommended for the prevention of worker injury and illness [11–14].

Currently, the most common standard analytical method for asbestos identification in bulk samples is polarized light microscopy (PLM) [15] and the method is used in several methods for the identification and quantification of asbestos that have been established by regulatory agencies [16–18]. However, there are known limitations of the technique. PLM relies on the knowledge of the microscopist, and misidentification including false positive, false negative, and asbestos identification errors can occur due to similarities in optical and morphological properties between asbestos and non-asbestos fibers [19, 20]. The resolution of light microscopy can limit the identification of the smallest asbestos fibers in some products. In addition, pretreatment such as heat and acid treatment can modify the refractive index of asbestos and induce alterations in its color [17,18,21]. Therefore, alternative methods are recommended for more accurate asbestos identification to be used in conjunction with PLM. Transmission electron microscopy (TEM) is often used to confirm asbestos identification; however, the instrument is expensive and requires a specialized laboratory with well-trained lab personnel for analysis [18,22]. Due to these operational limitations, there is growing need to introduce more accessible and cost-effective alternatives, such as FTIR spectroscopy.

Utilizing Fourier Transform Infrared (FTIR) can be an option for asbestos identification by providing known mineralogical information of samples [23–25] and may minimize human bias that is driven by the inherent subjectivity of interpreting optical properties when using PLM. In addition FTIR has been demonstrated to be a cost-effective, non-destructive technique with minimal sample preparation and fast analysis time [26–30]. Recently, Zholobenko *et al.* showed an application of vibrational spectrometers [FTIR, Near IR (NIR), and Raman] for asbestos detection in ACMs [31]. Swayze *et al.* have demonstrated the utility of IR spectroscopy for recognizing amphibole minerals in commercial vermiculite insulation products [32]. In addition, Lee *et al.* showed an application of FTIR spectrometry and multivariate data analysis for classification between six regulated asbestos and their non-asbestiform analogs. The samples from the study were laboratory generated with the well characterized reference materials but not real ACMs [33].

The present study was conducted to investigate a laboratory procedure for an asbestos identification tool in suspected bulk ACMs using the Diffuse Reflectance Infrared Fourier Transform (DRIFT) mode along with multivariate data analysis via Partial Least Squares-Discriminant Analysis (PLS-DA).

2. Materials and methods

2.1. Sample preparation for training data and FTIR measurement

Six regulated asbestos types were used for the model calibration (Table 1): 1) actinolite (National Institute for Standards and Technology (NIST) Standard Reference Materials (SRM), NIST SRM 1867), 2) Amosite (NIOSH, GF-38), 3) anthophyllite (NIOSH, AF-45), 4) chrysotile (NIOSH, CH-29), 5) Crocidolite (NIOSH, CR-36), and 6) tremolite (NIOSH, TF-48). The NIOSH reference materials were prepared and characterized to provide reference materials for the development of analytical methods [34] and the material have also been utilized in prior research studies [33–37]. All five NIOSH reference materials were milled to have a particle size distribution similar to that found in an occupational environment [34] except the NIST actinolite. The actinolite was ground using an XRD-Mill (McCrone Microscope and Accessories LLC) for 30 min, filtered, and dried for further preparation. Because the particle sizes may affect the FTIR absorption [38], a series of sieves (ASTM E-11 standards) with mesh sizes of 250 μm (No. 60) and 106 μm (No. 140) were employed to obtain a uniform sample size range (106–250 μm). The particle size range was chosen because preparation with relatively larger sizes might be easier compared to the smaller sizes (minimizing grinding). The mass of each asbestos type was determined using a microbalance (Mettler-Toledo, Columbus, OH, USA) and thoroughly mixed with potassium bromide (KBr, IR transparency) at a dilution ratio of 1:100 [39]. The total mixture mass of each sample was approximately 100 mg. A portion of the mixture was transferred to a sampling cup (10 mg capacity, ThermoFisher Scientific, Waltham, MA), and the sampling cup was placed in a cup holder inside of the diffuse reflectance accessory (COLLECTOR™ II, P/N 0030–0XXP, ThermoFisher Scientific) for FTIR measurement. FTIR spectra were obtained using a portable FTIR (Nicolet iS5, ThermoFisher Scientific) spectrometer equipped with a diffuse reflectance accessory. The application of DRIFT is designed to analyze geochemical composition and polymorphism with simple sample preparation steps [24,40,41]. The DRIFT technique captures the diffused scattered light of the sample that is focused on the detector through optical mirrors to generate a spectrum [42], and qualitative and quantitative asbestos analysis in bulk samples using the DRIFT technique have been demonstrated [43–46]. The conventional transmission mode requires more steps to prepare KBr pellets [40], adding uncertainty due to KBr pellet thickness variability and changing the structure of crystalline substances in the sample during pellet pressing [24]. The DRIFT technique was chosen because it allows direct analysis of asbestos and KBr mixtures with minimal preparation, avoiding the pressure induced structural changes that can occur during pellet preparation in transmission mode, and preserving the chemical and morphological integrity of the asbestos. The measured samples in

Table 1
Asbestos reference materials for PLS-DA model calibration.

Asbestos Type	Source	Reference number
Actinolite	NIST[+], Fairfax County, VA, USA	SRM 1867
Amosite	NIOSH*, Lydenburg, South Africa	GF−38
Anthophyllite	NIOSH*, Montana, USA	AF−45
Chrysotile	NIOSH*, Idria Range, CA, USA	CH−29
Crocidolite	NIOSH*, South Africa	CR−36
Tremolite	NIOSH*, Rajasthan, India	TF−48

[+]National Institute of Standards and Technology
*National Institute for Occupational Safety and Health

the sampling cup were placed back into the original mixture and mixed thoroughly for another FTIR measurement. Although the training spectra for each asbestos type were derived from the same mixture, they were not identical and spectral variation might arise between the samples due to slight differences in mass and ratio of asbestos to KBr. The OMNIC 9.7.46 software was used in a Kubelka–Munk mode at 4 cm^{-1} resolution by averaging 16 scans. For the training data, a total of 600 spectra were collected (100 spectra for each asbestos type) over the wavenumber range of 4000–400 cm^{-1}. Each day, an average of 10 blank potassium bromide (KBr) measurements was utilized as a background for the asbestos sample measurement.

2.2. Multivariate data analysis

PLS-DA (PLS_Toolbox, v8.9.1, Eigenvector Research Inc., Manson, WA) operating in MATLAB (The MathWorks, Inc.) was utilized to observe patterns of similarity within FTIR spectra from six asbestos types. PLS-DA is a statistical method for classification and discrimination tasks, commonly applied in fields such as pharmaceuticals, environmental monitoring, forensic science, food chemistry, and chemometrics [47,48]. PLS-DA models rely upon the FTIR wavenumber intensities along with the shape of the spectra and works to group the spectra based on relative similarity, and dissimilarity, to all other spectra in the training data. The samples with similar spectra will be closely clustered on a score plot, while the samples with dissimilar spectra will be clustered further apart. PLS-DA is an extension of partial least squares regression (PLS) and works by finding latent variables (LVs) that maximize the covariance between the predictor variables (X – FTIR data) and the class indicators (Y – asbestos type). These latent variables are then used to build a predictive model that classifies unknown samples into one of the predefined PLS-DA classes. The PLS-DA model was cross-validated using Venetian blinds with 10 splits and a blind thickness of 1 with a cross-validation class error average of 0 for each class of the training data. When cross-validating the model, the algorithm leaves out the class data from a subset of the data, then tries to predict the class and use the known class information to see if it correctly predicts the class. The data in the PLS-DA model was preprocessed via Savitzky–Golay 1st derivative (second order polynomial with a 15-wavenumber smoothing window), 1-normalization, followed by median centering before hierarchical cluster analysis via Ward's method and PLS-DA [49]. The spectral range of 400–1200 cm^{-1} wavenumbers was employed for training data. When analyzing the training data, the first five latent variables (LVs) were selective based on cross-validation results and cumulative explained variance (91.83 %), ensuring optimal model accuracy with the first LV accounting for 30.77 % and the second LV accounting for 29.49 % of the total variance in the data. Class error is defined as the average of false positive rate and false negative rate for each class (1 – (sensitivity + specificity)/2).

2.3. PLS-DA model evaluation

2.3.1. Laboratory generated challenge samples

In order to evaluate the PLS-DA model, three different groups of laboratory generated samples were prepared: 1) samples with the calibration samples (Table 1); 30 single asbestos samples (5 different samples for each asbestos type) and 45 samples of mixed two asbestos types with 1:1 mass-based ratio (3 different samples for 15 different pairs), 2) additional 19 different asbestos reference materials (Table 2) for FTIR spectra variation between the reference materials, 3) glass fibers and wollastonite as false negative samples (non-asbestos fibers). The preparation and analysis for each sample was the same as the calibration samples; mixed with KBr, measured with FTIR, and processed with PLS-DA.

2.3.2. Suspected ACM bulk samples

The suspected ACM bulk samples were from three different laboratories; 1) RJ Lee Group provided the ACM bulk samples collected from the remediation and/or building management industries and the samples contain either chrysotile or no asbestos. The ACM bulk samples were analyzed by PLM (Leica DM750P) following the U.S. EPA method 600/R-93/116 [17], 2) Research Triangle Institute International provided amphibole-containing bulk materials previously used for PLM proficiency testing of the National Voluntary Laboratory Accreditation Program (NVLAP) and the samples were analyzed by the US EPA method 600/R-93–116 [17], and 3) A laboratory in the United Kingdom provided four additional suspected ACMs collected from industrial facility (pipe insulations) and the samples were analyzed by a NIOSH contracted laboratory using PLM analysis (NIOSH method 9002) [21]. Visible fibers were extracted from the ACM bulk samples when possible and mixed with KBr for FTIR measurement (five different FTIR measurements for each sample). When fibers were not visible from the samples, a random portion of the sample was extracted and mixed with KBr. Further sample treatment including muffle furnace ashing and acid wash [22] were added when necessary (failure on a classification from the PLS-DA (unassigned) or no visible fibrous materials). The ashing process was conducted using a muffle furnace (MS Microtherm, Mellen Company, Concord, New Hampshire) for 2 h at 490°C to remove organic materials. Hydrochloric acid (25 %) was utilized to remove calcite in the samples.

2.3.3. Additional samples for particle size effect

Additional 25 samples of chrysotile (NIOSH, CH-29) and Amosite

Table 2
Other reference materials for PLS-DA prediction.

Reference materials	Source	PLS-DA prediction with all asbestos types	PLS-DA prediction with actinolite and tremolite only
Actinolite	Juneau, AK	Tremolite/ Crocidolite	Actinolite
	Goolwa Quarries, South Australia	Unassigned	Actinolite
Amosite	U.S. Bureau of Mines standard	Amosite	Not applicable
	NIST SRM1866b	Amosite	
Anthophyllite	Palm Springs, CA	Anthophyllite	
	NIST SRM1867a	Anthophyllite	
	Dadeville, AL	Anthophyllite	
Chrysotile	U.S. Bureau of Mines standard	Chrysotile	
	NIST-SRM1866b	Chrysotile	
Crocidolite	NIST-SRM1866b	Crocidolite	
	NIOSH, CR−37	Crocidolite	
	UICC, South Africa	Crocidolite	
	U.S. Bureau of Mines standard	Crocidolite	
	Wittenoom, Western Australia	Crocidolite	
Tremolite	Lone Pine, CA	Actinolite	Actinolite
	Barstow, CA	Tremolite	Tremolite
	Cemetery Ridge, CA	Unassigned	Tremolite
	CK Williams Quarry, Easton, PA	Unassigned	Actinolite/ Tremolite
	El Dorado County, CA	Unassigned	Tremolite

(NIOSH, GF-38) in smaller size (<53 μm) compared to the calibtration samples, were prepared for particle size effect on the FTIR measurement.

3. Results and discussion

3.1. Asbestos classification and prediction

FTIR DRIFT spectra of the asbestos reference samples within the range of 400–1200 cm^{-1} (Top) and the classification of asbestos types using calibration samples including the score plot generated with the first two latent variables (LVs) from the PLS-DA model (Bottom) are shown in Fig. 1. Although five LVs were used for prediction, the first two captured the most significant spectral differences. All asbestos types showed distinct clusters except actinolite and tremolite due to their similarities in peak positions in the FTIR spectra [46]. Each asbestos type has a threshold value (Y-predicted) based on the LVs. For an unknown sample to be assigned to an asbestos type, the prediction probability must exceed the threshold value. In PLS-DA, a Bayesian method is used to calculate the probability that a sample belongs to a class [50]. This is achieved by fitting a normal distribution to the predicted y-values for each class and then using that distribution to calculate the probability. The Y-predicted value of each asbestos type was around 0.5, except for Crocidolite which exhibited a lower threshold (0.2). However, the clear classification of each of the six asbestos types was observed, and the PLS-DA model can differentiate between the asbestos types. While various approaches exist for validating predictions of unknown samples using a PLS-DA model [51], the present study employed Y-predicted values in cross-validation prediction plots (above or below Y-predicted cut-off value) and Class Prediction Probability, either 0 (unassigned) or 1 (assigned an asbestos type(s)) for its classification.

Donut plots for actual sample composition and average Y-predicted values of asbestos compositions for challenge single asbestos samples are shown in Fig. 2. Each donut plot has the two highest Y-predicted values (%) of asbestos types and other types (the sum of predicted values (%) from all other asbestos types together). The Y-predicted values are an average of five individual Y-predicted values from five different FTIR measurements. The PLS-DA model accurately predicted the asbestos type for all challenge single asbestos samples based on two criteria: 1) above the Y-predicted cut-off value on the actual asbestos type and 2) correct Class Prediction Probability value (1) on the actual asbestos

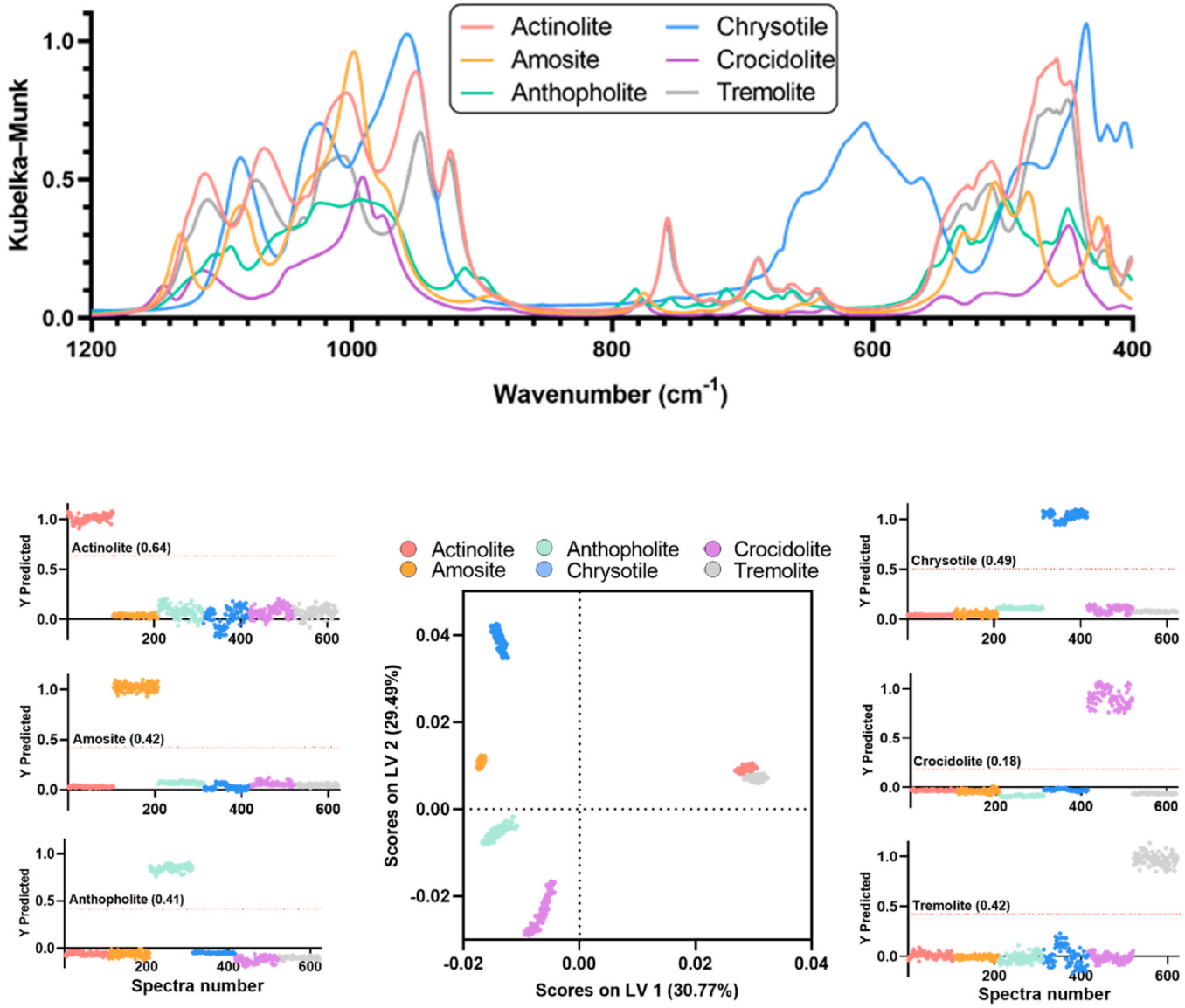

Fig. 1. Asbestos reference samples FTIR DRIFT spectra within the range of 400–1200 cm^{-1} (Top) and classification of asbestos types in the score plot (Bottom center) and cross-validation prediction plot with Y-predicted cut-off value of each asbestos type (Bottom).

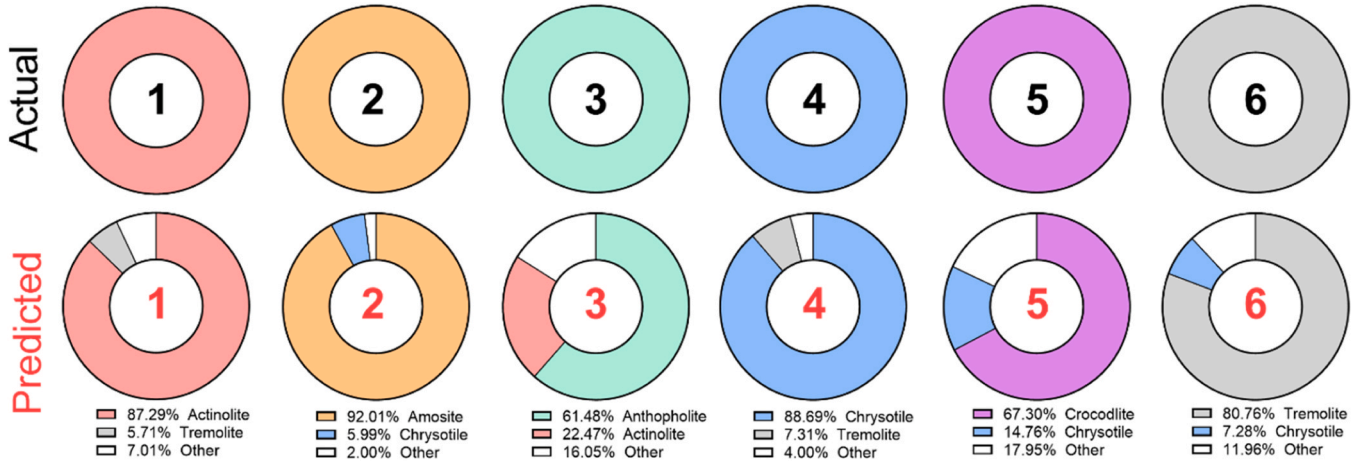

Fig. 2. Actual mass content (%) and averaged Y-predicted composition (%) of the asbestos types for a single asbestos sample.

type. The highest Y-predicted value was found in Amosite sample #2 (0.92), while the lowest Y-predicted value was found in the anthophyllite sample #3 (0.61).

Donut plots for actual sample mass content (%) and average Y-predicted values of asbestos compositions for mixed challenge samples are shown in Fig. 3. Each sample is a mixture of two asbestos types at a 1:1 mass-based ratio. Three individual samples for each sample were prepared and averaged. For all 15 mixed samples, the model correctly predicted two asbestos types (double assigned; Class Prediction Probabilities were 1 s on both asbestos types) except #4, #5, and #15. Samples #4, #5, and #15 were predicted as one asbestos type, actinolite, tremolite, and tremolite, respectively.

The present study utilized the NIOSH and NIST reference materials for six regulated asbestos types (Table 1). It is possible that even within the same asbestos type there may be variation within the FTIR spectrum between samples which are driven by compositional variability of the source deposits. For example, if two tremolite asbestos reference materials were collected from two different locations but clustered in different locations on a PLS-DA score plot, there would be a discernable effect of compositional variability within tremolite. If this were the case, the model would need to be built with all possible different reference materials from multiple locations in order to capture the range of compositional variability and would result in complications in the use of PLS-DA models for asbestos identification. PLS-DA model prediction for the additional 19 different asbestos reference materials are shown in Table 2. The model correctly predicted all reference materials except actinolite and tremolite. Another prediction was made with only actinolite and tremolite calibration samples, and PLS-DA was predicted correctly except for two samples (Lone Pine and CK Williams quarry).

The prediction of the PLS-DA for glass fiber samples [52] were unassigned (no asbestos found), while wollastonite was misclassified as tremolite. Zholobenko *et al.* included other materials that can be found in ACMs in the calibration procedure for a better identification [31]. When the wollastonite was included in the PLS-DA model (n = 100) as training data along with the six asbestos types and the PLS-DA, prediction was correct (data not shown). Calibrating the model with

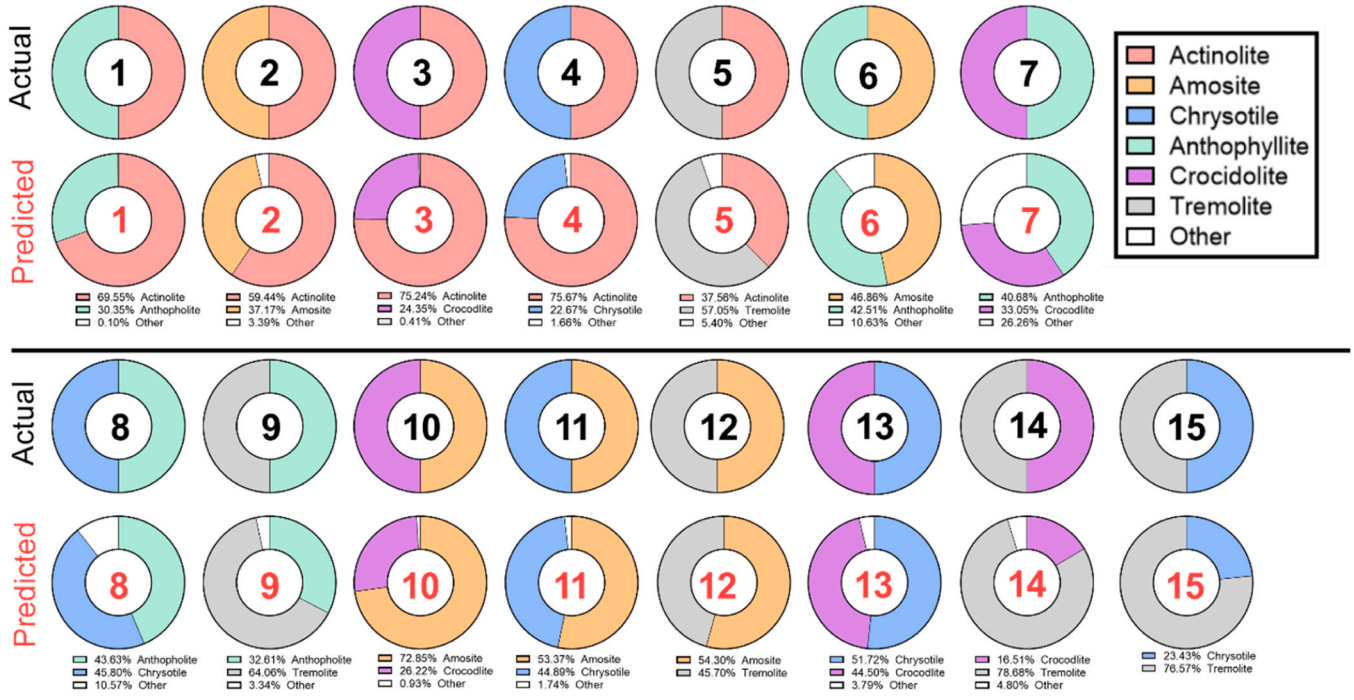

Fig. 3. Actual mass content (%) and averaged Y-predicted composition (%) of the asbestos types for mixed challenge samples.

interference or hierarchical modeling [53] are possible approaches that might be worth checking the model's prediction when other materials were included in the training process.

A box plot generated with Y-predicted values of 25 chrysotile-containing samples is shown in Fig. 4. Five different FTIR measurements for each sample were obtained. These samples were identified as chrysotile asbestos by PLM analysis with an estimated chrysotile content in the bulk materials ranging from 0.15 % to 90 %. These samples represent a cross-section of ACM building materials provided to a commercial laboratory for analysis found to be positive for asbestos by PLM and are predominantly comprised of flooring, roofing, and insulation materials. The median Y-predicted value of the training samples is 1.03. The Y-predicted values of samples #1–#20 were greater than the threshold value of chrysotile asbestos, and Class Prediction Probabilities were 1 s on chrysotile. However, Y-predicted values of 5 samples (#21–#25) were below the threshold value, and Class Prediction Probabilities were either 0 (unassigned) or 1 (other asbestos types, sample #23 assigned as Amosite and tremolite). Because most of the ACMs contain other materials such as rock wool, slag wool, fiberglass, gypsum, vermiculite, perlite, clay, calcite. [17], extra sample treatment (muffle furnace ashing and acid washing) for those 5 samples was conducted. After the muffle furnace ashing process, samples #21 and #22 were predicted as chrysotile. After both the ashing and acid-washing processes, samples #23 and #24 were predicted as chrysotile. However, sample #25 remained unassigned after the treatments. Adding the sample treatment steps in the procedure, especially the samples with no visible fibrous materials, might minimize the potential for interference with other materials in FTIR spectra and result in more accurate predictions. The prediction of the PLS-DA for 12 non-asbestos-containing bulk samples were unassigned (no asbestos found) and it remained unchanged after ashing and acid washing.

Donut plots for amphibole-containing bulk materials (1 actinolite, 2 Amosite, 2 anthophyllite, 1 Crocidolite, and 1 tremolite-containing material) with Y-predicted values of asbestos compositions are shown in Fig. 5. The amphibole samples are materials for an acid waste storage tank wall, block insulation, board insulation, and laboratory-generated samples, and estimated asbestos content in the bulk materials ranges from 1.1 % to 28 %. The PLM analysis results of anthophyllite (sample #1), Amosite (sample #2 and #3) and Crocidolite (sample #4) samples each agreed with the PLS-DA predictions. PLS-DA initially predicted unassigned for the samples of anthophyllite (sample #5, 3 %), tremolite (sample #6, 1.5 %), and actinolite (sample #7, 1.5 %), but both analysis results agreed after muffle furnace ashing and acid washing.

Donut plots of multiple asbestos-containing bulk samples with estimated percentages as analyzed by PLM and the Y-predicted values from the PLS-DA model are shown in Fig. 6. Chrysotile, Amosite, and Crocidolite were detected in all samples by the PLM analysis, and Y-predicted values from the PLS-DA partially align with the PLM analysis. The PLS-DA (Class Prediction Probability) predicted samples #1 as chrysotile and Crocidolite (double assigned), #2 as chrysotile, #3 as Amosite, and #4 as Amosite. It should be noted that the PLS-DA prediction was better with single asbestos-containing materials than with multiple asbestos-containing materials, which may need further evaluation.

3.2. Particle size and sample number for PLS-DA calibration

Twenty-five extra samples smaller than 53 μm of chrysotile and Amosite samples were prepared for particle size effect on the FTIR measurement, and no difference between particle sizes on PLS-DA prediction was found.

Because the Y-predicted values can be dependent on the sample number of the training samples, the Y-predicted values of challenge samples (single asbestos samples) were determined with various sample numbers of PLS-DA calibration samples (n = 100, 83, 66, 50, 33, 17, 8, 2 for each asbestos type). Although all the challenge samples were correctly predicted regardless of sample number, the overall Y-predicted value for each asbestos type was negatively affected when the sample number was decreased. This finding aligns with the idea that larger training datasets tend to enhance accuracy in all types of machine learning by reducing the chances of overfitting [54]. However, the optimal sample number using FTIR and PLS-DA for asbestos identification is still unknown and need to be more investigated; may be unique based on the specific needs of the modeling technique that is used.

3.3. KBr background effect

Although the model correctly predicted the single-class challenge samples, the challenge samples clustered a little off from the calibration samples on the score plot. In addition, the average Y-predicted value of chrysotile asbestos was around 70 % and it should be higher because the calibration and challenge samples are from the same material, and both have a similar mass ratio chrysotile to KBr. The average KBr background sample was obtained when the FTIR spectra for calibration samples were collected and the same background was used for challenge samples, which was attributable to the relatively lower Y-predicted composition levels due to day-to-day variations in temperature and relative humidity levels. The average KBr background sample was obtained for the day of the sample measurement and the average Y-predicted value level of the chrysotile was increased to 89 % (Fig. 2).

3.4. Limit of detection

To determine the limit of detection (LOD), around 100 mg of each

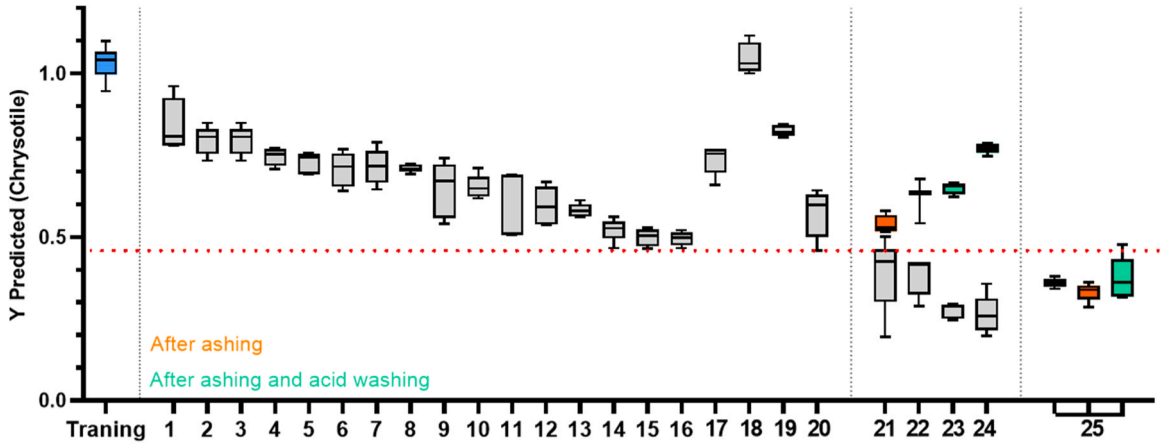

Fig. 4. Box plot of Y-predicted values for 25 chrysotile-containing samples along with Y-predicted cut-off value (red dotted line).

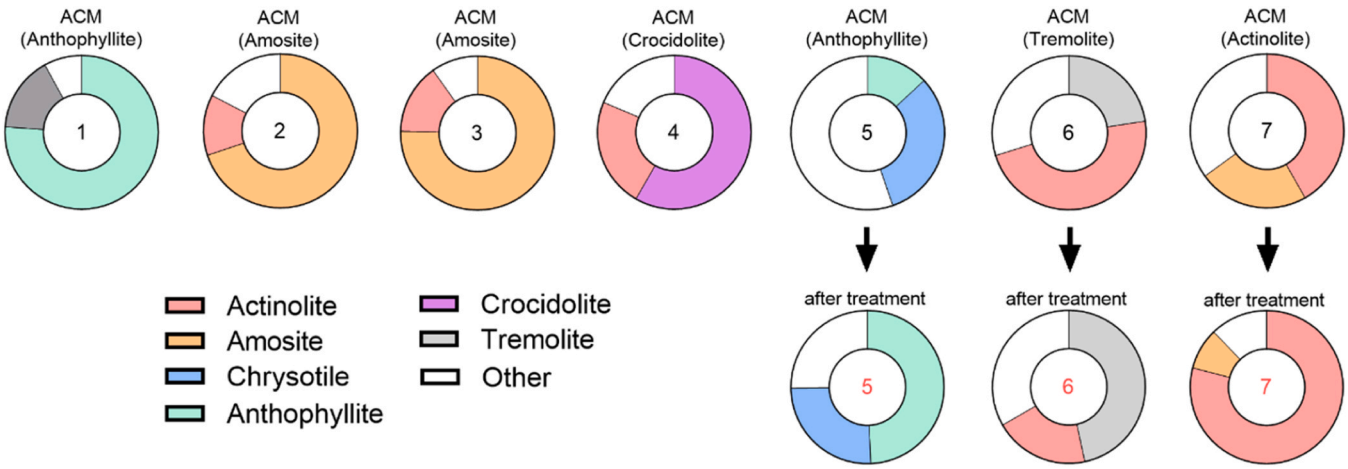

Fig. 5. Amphibole-containing bulk materials with Y-predicted values of asbestos compositions and changed Y-predicted values after pretreatment.

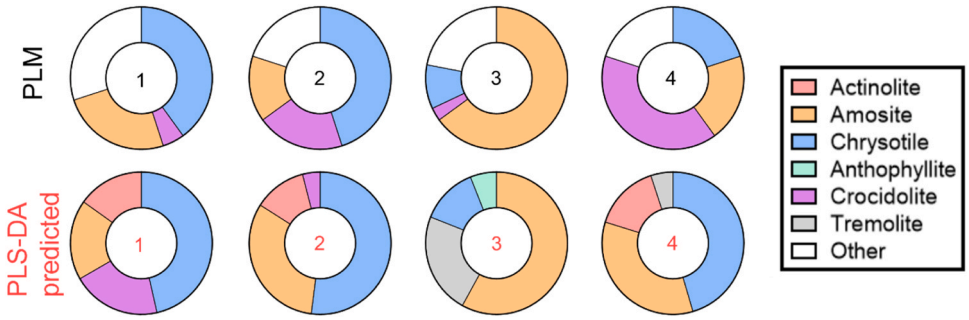

Fig. 6. PLM asbestos estimation (%) and Y-predicted values from the PLS-DA model of multiple asbestos-containing bulk samples.

type asbestos and KBr mixture samples were prepared with different mass-based % of asbestos to KBr (0.1, 0.025, 0.0063, and 0.0016 wt%). Because the sampling cup is not capable of holding 100 mg of the mixture sample, the asbestos mass in the sampling cup was estimated using the actual mass of the mixture sample determined by gravitational analysis and mass %. For each mass ratio, 25 FTIR spectra were obtained and processed with PLS-DA. The PLS-DA predictions were used to determine LODs; the lowest mass that the model predicted correctly. The estimated lowest masses that PLS-DA predicted correctly were 0.16 μg for tremolite, 0.22 μg for Crocidolite, 0.84 μg for Amosite, 0.86 μg for actinolite, 0.92 μg for chrysotile, and 3.96 μg for anthophyllite. It is important to note that the limit of detection (LOD) values in this study were determined using pure asbestos samples mixed with KBr under controlled laboratory conditions. As a result, the minimum detectable masses identified here may not directly correspond to the minimum detectable mass in a commercial asbestos-containing material (ACM) analyzed using this technique.

3.5. Limitation and strength of the method

Zholobenko *et al.* analyzed ACMs using NIR spectroscopy without any pretreatment procedure and fiber extraction and showed distinctive NIR spectra patterns in the wavenumber 7300–7000 cm^{-1} (O-H stretching vibrations) [31]. However, the present study extracted fibrous sections from the samples, and extra sample treatment steps were involved depending on the matrix of the material, indicating that extraction of the sample may not fully represent the entire ACMs, and additional samples from different sections of the ACM sample might be required. In addition, misclassification from the PLS-DA model can occur if the sample mass deviates significantly from the calibration data or if interference is raised from other materials in the 400–1200 cm^{-1} region. Additionally, using high-dimensional datasets for multiclass prediction, which are driven by the assumption of linearity and reduced into latent variables, makes understanding and interpreting the results challenging. The laboratory protocol presented here might be less dependent on the experience of the analyst compared to the microscope analysis by measuring unique chemical properties of the asbestos and it is cost-effective, rapid and sensitive. The PLS-DA model has demonstrated that specific interest minerals can be added to the calibration data, making it a valuable tool for asbestos identification and potentially for other elongated mineral particles (EMPs).

Based on the findings from the present study, a laboratory procedure of asbestos identification using FTIR and PLS-DA can be suggested, and it is shown in Fig. 7. The acid washing and ashing procedures were recommended when no asbestos was predicted with visible fibers

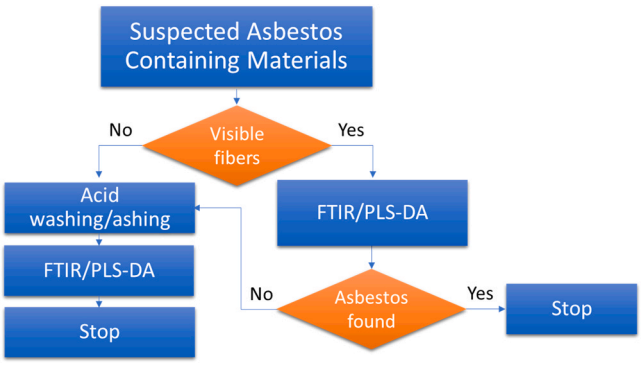

Fig. 7. A suggested laboratory procedure of asbestos identification in suspected asbestos-containing materials using FTIR and PLS-DA.

because asbestos and other materials could interfere with FTIR spectra.

4. Conclusion

FTIR combined with PLS-DA showed a rapid, cost-effective, and reliable procedure for identifying asbestos types in bulk samples. The model accurately classified single-asbestos samples and aligned with PLM analysis results. While PLS-DA model prediction with the multiple asbestos containing samples was less accurate, additional sample treatments improved accuracy. Further optimization through expanded datasets and model refinement is necessary.

Disclaimer

The findings and conclusions in this report are those of the authors and do not necessarily represent the official position of the National Institute for Occupational Safety and Health (NIOSH), Centers for Disease Control and Prevention (CDC). Mention of any company name or product does not constitute endorsement by NIOSH.

Environmental implication

This study developed and validated a laboratory method for identifying asbestos types in bulk materials using FTIR combined with multivariate data analysis. The method was tested on laboratory-generated asbestos-containing samples as well as on suspected ACMs collected from the remediation and building management sectors. This approach could serve as a complementary tool for asbestos detection in bulk samples together with other analysis methods including polarized light microscope and transmission electron microscope. While the method performs well for single asbestos containing samples, less accurate classification was found with multiple asbestos containing samples.

CRediT authorship contribution statement

Steven E Mischler: Writing – review & editing. **Salman Alquwayi:** Writing – review & editing, Writing – original draft, Investigation, Formal analysis, Data curation. **Taekhee Lee:** Writing – review & editing, Writing – original draft, Visualization, Supervision, Project administration, Methodology, Investigation, Formal analysis, Data curation, Conceptualization. **Sena Yang:** Writing – review & editing, Investigation, Formal analysis, Data curation. **Cody Wolfe:** Writing – review & editing, Visualization, Formal analysis, Data curation. **Bryan Bandli:** Writing – review & editing, Writing – original draft, Investigation, Formal analysis, Data curation.

Funding

The National Institute for Occupational Safety and Health (NIOSH), Project #9390M9B: Measurement and Analysis Tools for Elongate Mineral Particle Exposure in Mining.

Declaration of Competing Interest

The authors declare that they have no known competing financial interests or personal relationships that could have appeared to influence the work reported in this paper.

Acknowledgements

Special thanks to Mr. Todd Ennis from RTI International and Mr. Sufi Shariff from Continental Environmental Services who provided insight and ACMs.

Data availability

Data will be made available on request.

References

[1] Environmental Protection Agency (EPA). Biden-Harris Administration finalizes ban on ongoing uses of asbestos to protect people from cancer. 2024. (accessed July 20, 2024).
[2] World Health Organization. Asbestos: elimination ofasbestos-related diseases. 2014. ⟨https://iris.who.int/bitstream/handle/10665/340579/WHO-FWC-PHE-EPE-14.01-eng.pdf?sequence=1⟩ (accessed ↱May ↱13, ↱2024).
[3] Stanaway, J.D., Afshin, A., Gakidou, E., Lim, S.S., Abate, D., Abate, K.H., et al., 2018. Global, regional, and national comparative risk assessment of 84 behavioural, environmental and occupational, and metabolic risks or clusters of risks for 195 countries and territories, 1990–2017: a systematic analysis for the global burden of disease study 2017. Lancet 392 (10159), 1923–1994. https://doi.org/10.1016/S0140-6736(18)32225-6.
[4] Furuya, S., Chimed-Ochir, O., Takahashi, K., David, A., Takala, J., 2018. Global asbestos disaster. Int J Environ Res Public Health 15 (5), 1000.
[5] van Zandwijk, N., Reid, G., Frank, A.L., 2020. Asbestos-related cancers: the 'Hidden Killer' remains a global threat. Expert Rev Anticancer Ther 20 (4), 271–278. https://doi.org/10.1080/14737140.2020.1745067.
[6] Wild, C., Weiderpass, E., Stewart, B.W., 2020. World cancer report: cancer research for cancer prevention. International Agency for Research on Cancer.
[7] Fazzo, L., Binazzi, A., Ferrante, D., Minelli, G., Consonni, D., Bauleo, L., et al., 2021. Burden of mortality from asbestos-related diseases in Italy. Int J Environ Res Public Health 18 (19), 10012.
[8] Thives, L.P., Ghisi, E., Thives Júnior, J.J., Vieira, A.S., 2022. Is asbestos still a problem in the world? A current review. J Environ Manag 319, 115716. https://doi.org/10.1016/j.jenvman.2022.115716.
[9] Cherian, S.V., Kumar, A., de Groot, P.M., Truong, M.T., Moran, C.A., 2023. Pneumoconiosis. In The Thorax: Medical, Radiological, and Pathological Assessment. Springer, pp. 693–710.
[10] Asbestos, I., 2012. Arsenic, metals, fibres, and dusts IARC monographs on the evaluation of carcinogenic risks to humans volume 100C. IARC/WHO C 100.
[11] Asbestos, 2011. Fibers and other elongate mineral particles: state of the science and roadmap for research. Current Intelligence Bulletin 62, DHHS Publication No. 2011-159. Department of Health and Human Services, National Institute for Occupational Safety and Health, Washington, DC.
[12] Bloise, A., Ricchiuti, C., Lanzafame, G., Punturo, R., 2020. X-ray synchrotron microtomography: a new technique for characterizing chrysotile asbestos. Sci Total Environ 703, 135675.
[13] Bloise, A., Ricchiuti, C., Punturo, R., Pereira, D., 2020. Potentially toxic elements (PTEs) associated with asbestos chrysotile, tremolite and actinolite in the calabria region (Italy). Chem Geol 558, 119896.
[14] Bloise, A., Kusiorowski, R., Lassinantti Gualtieri, M., Gualtieri, A.F., 2017. Thermal behaviour of mineral f ibres. In: Gualtieri, A.F. (Ed.), Mineral Fibres: Crystal Chemistry, Chemical-Physical Properties, Biological Interaction and Toxicity, 18. European Mineralogical Union, London, UK, pp. 215–252.
[15] Quality, A., 2012. Bulk materials–Part 1: sampling and qualitative determination of asbestos in commercial bulk materials. NF ISO, 22262-22261.
[16] Works-Serials, C., 1987. Asbestos-containing materials in schools; final rule and notice (CIT). In: Part III: Environmental Protection Agency. 40 CFR Part 763, 52. INSTITUTION Environmental Protection Agency, Washington, DC PUB DATE 30 Oct 87, p. n210 (CIT).
[17] Environmental Protection Agency (EPA), 1993. Method for the determination of asbestos in bulk building material. EPA/600. R-93-116. US Environmental Protection Agency, Report.
[18] Occupational Safety and Health Administration (OSHA), C., Daniel T. Sampling and analytical methods: polarized light microscopy of asbestos. Department of labor,Branch of Physical Measurements and Analysis, OSHA Salt Lake Technical Center, Salt Lake City, Utah 84165-0200 1992; Vol. ID-191.
[19] Webber, J.S., Carhart, L.J., Czuhanich, A.G., 1997. Analytical trends in asbestos analysis: New York State's bulk sample proficiency-testing program. Am Ind Hyg Assoc J 58 (11), 809–813. https://doi.org/10.1080/15428119791012315.
[20] Harvey, B.W., Winstead, W.G., 2008. Analysis of the analytical performance of laboratories participating in two major US bulk asbestos proficiency testing programs. J Occup Environ Hyg 5 (7), 455–462.
[21] National Institute for Occupational Safety and Health (NIOSH). ASBESTOS (bulk) by PLM 9002. Fourth Edition ed.; NIOSH Manual of Analytical Methods (NMAM): 1994; Vol. RTECS: C16475000.
[22] Ham, S., Hwang, S., Yoon, C., 2019. Comparison of methods for pretreatment and quantification of bulk asbestos samples for polarized light microscopy analysis to evaluate asbestos-containing waste. Sustainability 11 (22), 6440.
[23] Sakaguchi, I., Kouketsu, Y., Michibayashi, K., Wallis, S.R., 2020. Attenuated total reflection infrared (ATR–IR) spectroscopy of antigorite, chrysotile, and lizardite. J Mineral Petrol Sci 115 (4), 303–312.
[24] Tkachenko, Y., Niedzielski, P., 2022. FTIR as a method for qualitative assessment of solid samples in geochemical research: a review. Molecules 27 (24), 8846.
[25] Gualtieri, A.F., Gandolfi, N.B., Passaglia, E., Pollastri, S., Mattioli, M., Giordani, M., et al., 2018. Is fibrous ferrierite a potential health hazard? Characterization and comparison with fibrous erionite. Am Mineral 103 (7), 1044–1055. https://doi.org/10.2138/am-2018-6508.

[26] Gadsden, J., Parker, J., Smith, W., 1970. Determination of chrysotile in airborne asbestos by an infra-red spectrometric technique. Atmos Environ (1967) 4 (6), 667–670.
[27] Beckett, S., Middleton, A., Dodgson, J., 1975. The use of infrared spectrophotometry for the estimation of small quantities of single varieties of UICC asbestos. Ann Occup Hyg 18 (4), 313–320.
[28] Patterson, J., O'Connor, D., 1966. Chemical studies of amphibole asbestos. I. structural changes of heat-treated crocidolite, amosite, and tremolite from infrared absorption studies. Aust J Chem 19 (7), 1155–1164.
[29] Iezzi, G., Della Ventura, G., Bellatreccia, F., Lo Mastro, S., Bandli, B.R., Gunter, M. E., 2007. Site occupancy in richterite-winchite from libby, Montana, USA, by FTIR spectroscopy. In: Mineralogical Magazine, 71. From Cambridge University Press Cambridge Core, pp. 93–104. https://doi.org/10.1180/minmag.2007.071.1.93.
[30] Hawthorne, F.C., Della Ventura, G., Oberti, R., Robert, J.-L., Iezzi, G., 2005. Short-range order in minerals: amphiboles. Can Mineral 43 (6), 1895–1920. https://doi.org/10.2113/gscanmin.43.6.1895 (acccessed 10/31/2024).
[31] Zholobenko, V., Rutten, F., Zholobenko, A., Holmes, A., 2021. In situ spectroscopic identification of the six types of asbestos. J Hazard Mater 403, 123951.
[32] Swayze, G.A., Lowers, H.A., Benzel, W.M., Clark, R.N., Driscoll, R.L., Perlman, Z.S., et al., 2018. Characterizing the source of potentially asbestos-bearing commercial vermiculite insulation using in situ IR spectroscopy. Am Miner J Earth Planet Mater 103 (4), 517–549.
[33] Lee, T., Mischler, S.E., Wolfe, C., 2024. Classification of asbestos and their nonasbestiform analogues using FTIR and multivariate data analysis. J Hazard Mater, 133874.
[34] National Institute for Occupational Safety and Health (NIOSH), 1979. Preparation and characterization of analytical reference minerals. Department of Health, Education, and Welfare. Public Health Service, Center for Disease Control, National Institute for Occupational Safety and Health.
[35] Morgan, A. From mines in the Coalinga region of California and from Quebec and British Columbia 1997.
[36] Silvestri, S., Di Benedetto, F., Raffaelli, C., Veraldi, A., 2016. Asbestos in toys: an exemplary case. Scand J Work Environ Health 80–85.
[37] Lee, T., Walker, R., Hummer, J., Ashley, E., Mischler, S., 2021. Size separation of amosite by filtration and shaking methods. Asbestos Other elongate Miner Part N Contin Chall 21st Century 1632, 265.
[38] Foster, R.D., Walker, R.F., 1984. Quantitative determination of crystalline silica in respirable-size dust samples by infrared spectrophotometry. Analyst 109 (9), 1117–1127.
[39] Coates, J., 1998. A review of sampling methods for infra red. Appl Spectrosc a Compact Ref Pract 49.
[40] Chen, Y., Zou, C., Mastalerz, M., Hu, S., Gasaway, C., Tao, X., 2015. Applications of micro-Fourier transform infrared spectroscopy (FTIR) in the geological sciences—a review. Int J Mol Sci 16 (12), 30223–30250.
[41] Le Pevelen, D., Tranter, G., 2017. FT-IR and Raman spectroscopies, polymorphism applications. Encycl Spectrosc Spectrom 750–761.
[42] Larkin, P.J., 2018. Chapter 3 - instrumentation and sampling methods. In: Larkin, P.J. (Ed.), Infrared and Raman Spectroscopy (Second Edition). Elsevier, pp. 29–61.
[43] Lang, P.L., Chu, V.-V., McCune, K., Franssen, S., Goodnight-Schmidt, M., Mendenhall, R., et al., 1998. Quantitation of asbestos using diffuse reflection infrared spectroscopy. Appl Spectrosc 52 (2), 212–217.
[44] Accardo, G., Cioffi, R., Colangelo, F., d'Angelo, R., De Stefano, L., Paglietti, F., 2014. Diffuse reflectance infrared Fourier transform spectroscopy for the determination of asbestos species in bulk building materials. Materials 7 (1), 457–470.
[45] Scardina, P.A.T. Quantitative determination of common types of asbestos by diffuse reflectance FTIR. 2013. ⟨https://www.agilent.com/library/applications/5991-3074ENE_high.pdf⟩ (accessed 8/16/2024).
[46] Ventura, G.D., Vigliaturo, R., Gieré, R., Pollastri, S., Gualtieri, A.F., Iezzi, G., 2018. Infra red spectroscopy of the regulated asbestos amphiboles. Minerals 8 (9). https://doi.org/10.3390/min8090413.
[47] Héberger, K., 2008. Chemoinformatics—multivariate mathematical–statistical methods for data evaluation. Medical applications of mass spectrometry. Elsevier, pp. 141–169.
[48] Barker, M., Rayens, W., 2003. Partial least squares for discrimination. J Chemom A J Chemom Soc 17 (3), 166–173.
[49] Zimmermann, B., Kohler, A., 2013. Optimizing Savitzky-Golay parameters for improving spectral resolution and quantification in infrared spectroscopy. Appl Spectrosc 67 (8), 892–902. https://doi.org/10.1366/12-06723.
[50] Pérez, N.F., Ferré, J., Boqué, R., 2009. Calculation of the reliability of classification in discriminant partial least-squares binary classification. Chemom Intell Lab Syst 95 (2), 122–128. https://doi.org/10.1016/j.chemolab.2008.09.005.
[51] Lee, L.C., Liong, C.-Y., Jemain, A.A., 2018. Partial least squares-discriminant analysis (PLS-DA) for classification of high-dimensional (HD) data: a review of contemporary practice strategies and knowledge gaps. Analyst 143 (15), 3526–3539.
[52] Lee, T., Ku, B.K., Walker, R., Kulkarni, P., Barone, T., Mischler, S., 2020. Aerodynamic size separation of glass fiber aerosols. J Occup Environ Hyg 17 (6), 301–311.
[53] Voccio, R., Malegori, C., Oliveri, P., Branduani, F., Arimondi, M., Bernardi, A., et al., 2024. Combining PLS-DA and SIMCA on NIR data for classifying raw materials for tyre industry: a hierarchical classification model. Chemom Intell Lab Syst 250, 105150.
[54] Belay, T.K., Dagnachew, B.S., Boison, S.A., Ådnøy, T., 2018. Prediction accuracy of direct and indirect approaches, and their relationships with prediction ability of calibration models. J Dairy Sci 101 (7), 6174–6189. https://doi.org/10.3168/jds.2017-13322.